

# RSC Advances



This is an *Accepted Manuscript*, which has been through the Royal Society of Chemistry peer review process and has been accepted for publication.

*Accepted Manuscripts* are published online shortly after acceptance, before technical editing, formatting and proof reading. Using this free service, authors can make their results available to the community, in citable form, before we publish the edited article. This *Accepted Manuscript* will be replaced by the edited, formatted and paginated article as soon as this is available.

You can find more information about *Accepted Manuscripts* in the [Information for Authors](#).

Please note that technical editing may introduce minor changes to the text and/or graphics, which may alter content. The journal's standard [Terms & Conditions](#) and the [Ethical guidelines](#) still apply. In no event shall the Royal Society of Chemistry be held responsible for any errors or omissions in this *Accepted Manuscript* or any consequences arising from the use of any information it contains.

## Flame-retardant, Flexible Vermiculite-Polymer Hybrid Film

Jun Young Cheong<sup>1</sup>, Jaehwan Ahn<sup>1</sup>, Mintae Seo<sup>1</sup>, and Yoon Sung Nam<sup>1,2,\*</sup>

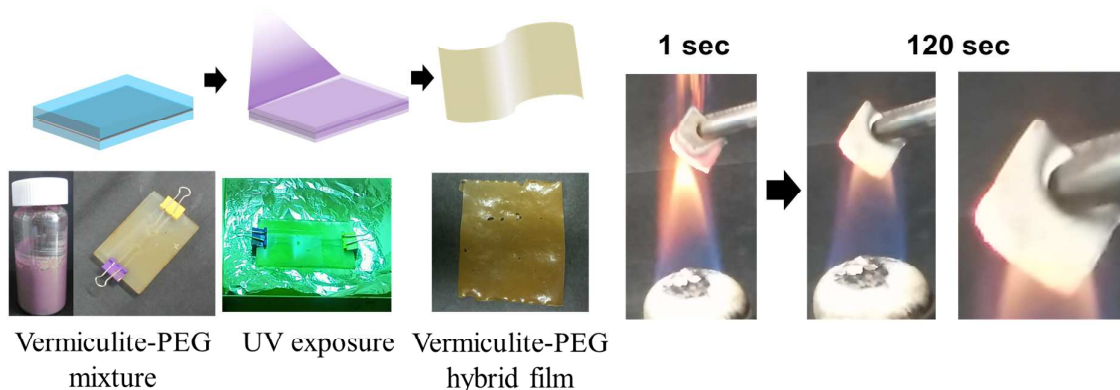
<sup>1</sup>Department of Materials Science and Engineering and

<sup>2</sup>KAIST Institute for NanoCentury (KINC CNiT),

Korea Advanced Institute of Science and Technology,

291 Daehak-ro, Yuseong-gu, Daejeon, 305-701, Republic of Korea

\*To whom all correspondence should be addressed (Email: yoonsung@kaist.ac.kr)



### Abstract

Flame-retardant, flexible polymer thin film and coating materials are in large demand for various applications. Three approaches have been attempted: inherently fire-retardant polymers; chemically modified polymers; and the addition of fire retardants as additives for polymers. The first two approaches are based on specific polymers, limiting their wide applications. The last approach provides great flexibility in designing materials with multifunctional properties. Herein, we report the fabrication of a flexible vermiculite-polymer hybrid film with very low flammability through photo-cross-linking of polyethylene glycol network incorporating micronized vermiculite particles. Vermiculite is a thermally insulating agent that can withstand flame up to about 1200 °C. The film fabrication process is very simple, time-efficient, and thickness-controllable. Despite quick processing of the film, vermiculite particles are uniformly distributed within the polymer network. Direct fire testing proves that, at a vermiculite concentration of about 75 wt-%, the films of 20 μm thick can withstand actual fire for more than a minute. Without vermiculite, the polymer film is burnt out immediately when in contact with flame. This study demonstrates that a vermiculite-polymer hybrid film, though it is relatively thin and highly flexible, can suppress the heat flow without decomposition for more than just a brief moment when in direct contact with flame.

Keywords: vermiculite; flame-retardant material; polyethylene glycol dimethacrylate (PEGDMA); UV polymerization; eco-friendly



## Flame-retardant, Flexible Vermiculite-Polymer Hybrid Film

Jun Young Cheong<sup>a</sup>, Jaehwan Ahn<sup>a</sup>, Mintae Seo<sup>a</sup>, and Yoon Sung Nam<sup>a,b,\*</sup>

Received 00th January 20xx,  
Accepted 00th January 20xx

DOI: 10.1039/x0xx00000x

www.rsc.org/

Flame-retardant, flexible polymer thin film and coating materials are in large demand for various applications. Three approaches have been attempted: inherently fire-retardant polymers; chemically modified polymers; and the addition of fire retardants as additives for polymers. The first two approaches are based on specific polymers, limiting their wide applications. The last approach provides great flexibility in designing materials with multifunctional properties. Herein, we report the fabrication of a flexible vermiculite-polymer hybrid film with very low flammability through photo-cross-linking of polyethylene glycol network incorporating micronized vermiculite particles. Vermiculite is a thermally insulating agent that can withstand flame up to about 1200 °C. The film fabrication process is very simple, time-efficient, and thickness-controllable. Despite quick processing of the film, vermiculite particles are uniformly distributed within the polymer network. Direct fire testing proves that, at a vermiculite concentration of about 75 wt-%, the films of 20 μm thick can withstand actual fire for more than a minute. Without vermiculite, the polymer film is burnt out immediately when in contact with flame. This study demonstrates that a vermiculite-polymer hybrid film, though it is relatively thin and highly flexible, can suppress the heat flow without decomposition for more than just a brief moment when in direct contact with flame.

### 1. Introduction

Fire/flame-retardant materials have served to protect materials or constructions from fire explosion and burning, which are crucially related to safety issues. Recently, researches on different chemicals have emerged for eco-friendly fire-retardant materials, some of which are chitosan phosphate,<sup>1</sup> melamine and its salts,<sup>2</sup> and starch-based chemical substances.<sup>3</sup> These eco-friendly fire-retardant products can be framed into different designs, such as fibers<sup>1,4,5</sup> and biodegradable materials,<sup>3,6</sup> in addition to a separator film.<sup>7</sup> Nevertheless, some drawback exists for these biochemical-based materials: either the fabrication process involves multi-steps or it is not fire-resistant to the actual flame.

With these limitations, inorganic materials have also been investigated. Vermiculite ((MgFe,Al)<sub>3</sub>(Al,Si)<sub>4</sub>O<sub>10</sub>(OH)<sub>2</sub>·4H<sub>2</sub>O), a hydrous silicate mineral, has been known for its inherent flame-retarding properties.<sup>8,9</sup> It has a triclinic structure and forms as a layered structure of minerals and water molecules. One important characteristic of bulk vermiculite is its exfoliated structure: when bulk vermiculite is heated at an elevated temperature (e.g., > 200 °C), exfoliation occurs through loss of water in the sheet interlayers and adapt to the elevated heat.<sup>10</sup> The main flame retardation mechanism of vermiculite lies in the self-intumescent properties

through exfoliation that passively inhibits thermal transfer when it is exposed to the heat flow.<sup>11,12</sup> Due to its resistance to structural decomposition, soil-compatible characteristics, and relatively low-cost, vermiculite has also been used in a variety of applications for the past 10 decades, such as a natural sorbent for heavy metals,<sup>13</sup> thermal energy storage materials,<sup>14</sup> a siloxane remover from biogas,<sup>15</sup> a soil conditioner,<sup>16</sup> brake pads,<sup>17</sup> anti-bacterial materials,<sup>18</sup> cements,<sup>19</sup> and an enhanced dechlorinator.<sup>20</sup> Among the different applications, it was used predominantly as a soil conditioner, in accordance with its biocompatible properties with the soil. Since soil is composed of different kinds of minerals, including silicate minerals and generally has a melting temperature above 1500 °C, it demonstrates inherent thermal stability. As vermiculite is one of the natural minerals found in soil,<sup>21-23</sup> its thermal stability is also somewhat analogous with that of soil.

With its heat-resistant characteristics, vermiculite has been proven to be an effective flame-retardant material and applied to flame-resistant lignocellulosic-mineral composites,<sup>24</sup> siloxane-based composites,<sup>25</sup> polypropylene composites,<sup>26-28</sup> and water-based acrylic fire retardant coating formulations.<sup>29</sup> Until now, vast majority of research dealt with either making composite materials and coating formulation or fabricating a hybrid film by multi-step and time-consuming procedures (longer than six hours). As a result, there is still limited research in the manufacturing of a thin, thickness-controllable (20 - 140 μm), and easily processed vermiculite film. Constant demand for such a thin, fast and efficiently processed film is present, ranging from energy harvesting material to simply preventing certain materials from catching on fire.

In this work, we introduce a simple method to fabricate a fire-retardant vermiculite-polymer hybrid film through photo-initiated

<sup>a</sup> Department of Materials Science and Engineering, Korea Advanced Institute of Science and Technology, 291 Daehak-ro, Yuseong-gu, Daejeon, 305-701, Republic of Korea.

<sup>b</sup> KAIST Institute for NanoCentury (KINC CNIT), Korea Advanced Institute of Science and Technology, 291 Daehak-ro, Yuseong-gu, Daejeon, 305-701, Republic of Korea.

\* E-mail: yoonsung@kaist.ac.kr

polymerization of polyethylene glycol macromers mixed with micronized vermiculite. For a vermiculite sample, South African vermiculite was used, devoid of asbestos contamination controversy as in the case of some other kinds.<sup>10,30,21,32,33</sup> To create a simple fabrication process of a film, poly(ethylene glycol) (PEG) macromers were mixed with vermiculite in ethanol and cross-linked into a polymer network by ultraviolet (UV) light-initiated polymerization with a photoinitiator.<sup>34-35</sup>

## 2. Experimental Section

### 2.1 Materials

Vermiculite from South Africa was obtained from Shinsung Mineral Co., Ltd (Sungnam, Republic of Korea). Poly(ethylene glycol)<sub>n</sub> dimethacrylate (PEGDMA) ( $n = 1000$ ) was purchased from Poly-science, Inc (Warrington, PA, USA). Ethanol was obtained from Daejung (Siheung, Republic of Korea). 2-Hydroxy-2-methyl-propiophenone (Darocur 1173) was purchased from Sigma-Aldrich (St. Louis, MO, USA). Micro slide glasses (76 mm × 52 mm) were obtained from Matunami glass Ind., Ltd (Kishiwada, Osaka, Japan). Trimethoxy(1H,1H,2H,2H-heptadeca-fluorodecyl)silane (THFS) was obtained from Tokyo Chemical Industry (Tokyo, Japan).

### 2.2 Glass surface treatment

Surface of the glasses was activated by oxygen plasma (Bioforce Nanoscience, Ames, IA, USA) for 30 min after surface washing with deionized water by sonication. The pre-treated glasses were immersed in 1 vol-% THFS for 1 h and thoroughly washed with 70 % ethanol.

### 2.3 Fabrication of vermiculite-PEG hybrid film

The fabrication process of a vermiculite-PEG hybrid film and its photometric images for easier understanding are shown in Fig. 1. A vermiculite-PEG hybrid film was prepared using micronized vermiculite particles, PEGDMA as a polymer, Darocur 1173 as a photo-initiator, and ethanol as a solvent. PEGDMA (80 mg) and

Darocur 1173 (10 mg) were dissolved in ethanol (110 mg) in a 20 mL glass vial. Darocur 1173 was used to initiate the photo-induced radical polymerization of PEGDMA. Micro-sized vermiculite and PEGDMA were mixed together with different weight ratios starting from 52.6 % to 69.0 % to 74.3 % at maximum for the preparation of a vermiculite-PEG hybrid film. The final mixed solution was cast between two silane-treated glass plates and transferred to a UV chamber. The solution was irradiated by a UV curing machine (DXF 1000, Republic of Korea, 365 nm, 400 W) for 10 min to prepare a fully cross-linked hybrid film. The thickness of the vermiculite-PEG hybrid film was controlled from 20  $\mu\text{m}$  to 140  $\mu\text{m}$  with degree of pressing on glass plate or attaching tapes or picking up with two small binder clips. The vermiculite-PEG hybrid film was dried for one day to evaporate ethanol in the film before it was analyzed.

### 2.4 Characterization

Thermal properties were measured using a thermogravimetry analyzer (TGA) (TG 209 F3, Netzsch, Germany and Labsys. Evo, Setaram, France). The decomposition of the prepared vermiculite-polymer composites and pristine vermiculite particles from 20 to 800 °C was determined with 20 °C min<sup>-1</sup> under argon flow. Thermal stability and the presence of melting point ( $T_m$ ) for vermiculite-PEG film below 240 °C was determined using differential scanning calorimetry (DSC) (DSC 204 F1, Netzsch, Germany) at a heating rate of 10 °C min<sup>-1</sup> under argon flow. The surface morphology of the vermiculite-PEG hybrid film was examined using scanning electron microscopy (SEM) (XL 30 S FEG, Philips, Netherlands) with a beam voltage of 10.0 kV. The image was taken for the front and backside of film and the cross-section of the film. The thickness of the vermiculite-PEG hybrid films was measured using a Vernier caliper. Energy-dispersive X-ray (EDX) spectroscopy was taken using field emission scanning electron microscopy (FE-SEM) (Magellan 400, FEI, USA) with a beam voltage of 10.0 kV. To examine the surface morphology of vermiculite particles after sieving (sieved vermiculites) and dispersion of vermiculite particles in the hybrid film, transmission electron microscopy (TEM) (JEM 3010, JEOL, Japan) images were taken. To examine the chemical

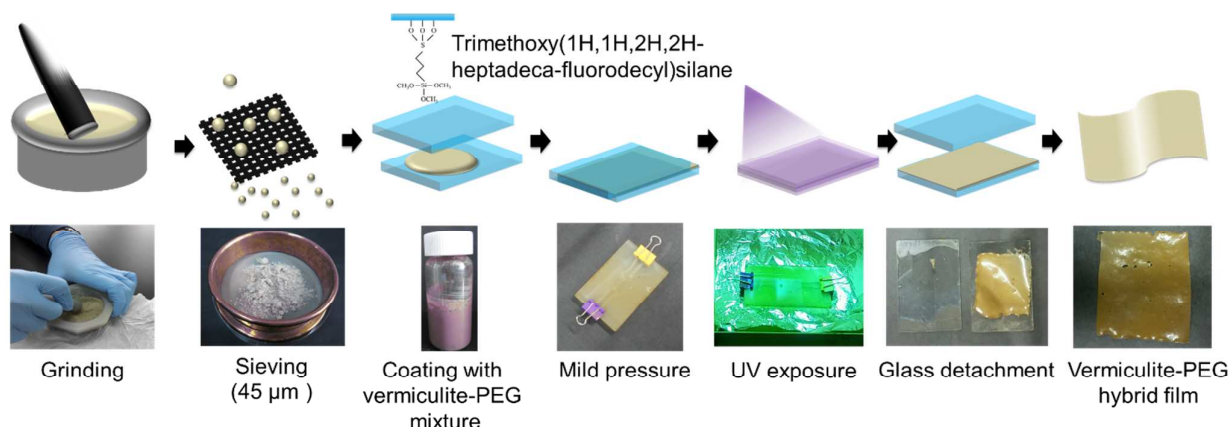


**Fig. 1.** Schematic description and photographic images of the fabrication process of a vermiculite-PEG hybrid film. Raw materials of commercial vermiculite were ground and put in a sieve of 45  $\mu\text{m}$  mesh size. Vermiculite-PEG solution was dropped on the THFS-treated glass slide and was sandwiched by two glass slides with mild pressure. After UV exposure for 10 min, a flexible vermiculite-PEG hybrid film can be obtained.

interactions between vermiculite and PEG, Fourier transform infrared (FTIR) (Nicolet iS50, Thermo Scientific, USA) analysis was carried out in a wavenumber ranging from 400 to 4000  $\text{cm}^{-1}$ . Lastly, to determine the mechanical properties of PEG film and vermiculite-PEG film, stress-strain curves were measured by a universal testing machine (UTM) (INSTRON 5583, Instron Co., USA).

### 2.5 Fire endurance testing of vermiculite-PEG hybrid films

As for the fire endurance tests, an alcohol lamp was prepared along with a lighter and fire was ignited on an alcohol lamp and rectangular part (1 cm  $\times$  1 cm) of each sample was put on fire fixed with the pincet. The fire endurance testing was performed for more than two minutes with respect to the thickness of the vermiculite-PEG hybrid film and the concentration of the vermiculite in the film of 20  $\mu\text{m}$  thick.

## 3. Results and Discussion

The compositions of three prominent vermiculite-PEG hybrid films are summarized in Table 1. These samples are denoted S1, S2, and S3, for our convenience. The diameter of original vermiculite was in the range of 0.3 mm - 0.7 mm (Fig. 2A). To obtain the desired diameter of a particle, which is roughly less than 45  $\mu\text{m}$  in diameter, vermiculite particles were ground in a bowl for several hours and sieved with 45  $\mu\text{m}$  mesh size of a sieve, as shown in Fig. 2B. Upon careful addition of sieved vermiculite particles (cutoff = 30  $\mu\text{m}$ ) to the solution composed of PEGDMA and ethanol in the presence of Darocur 1173, 74 wt-% of vermiculite was the maximum amount, at which the vermiculite-PEG hybrid films were successfully made. Theoretical weight percentage of vermiculite after UV curing was calculated based on the assumption that ethanol would be completely evaporated and that Darocur 1173 would help to cross-link the PEGDMA well with the vermiculite powders.

As the S3 sample was expected to exhibit the best fire-retardant effects, the surface morphology of the S3 sample was analyzed using SEM. To confirm the accuracy of the morphology, different set of SEM images was taken in multiple different points, with front and backsides of the film, as shown in Fig. 3. The observation between

**Table 1.** Compositions of three representative vermiculite-PEG hybrid films.

Sample #	Vermic-ulite	PEG-DMA	Ethanol	Daro-cur 1173	Weight percentage of vermiculite
S1	100 mg	80 mg	110 mg	10 mg	52.6 %
S2	200 mg	80 mg	110 mg	10 mg	69.0 %
S3	260 mg	80 mg	110 mg	10 mg	74.3 %

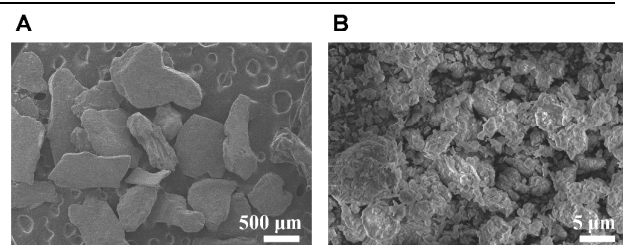


**Fig. 2.** SEM image of (A) raw material of commercial vermiculite and (B) vermiculite particles after sieving

This journal is © The Royal Society of Chemistry 20xx

front and back side of film indicates that no significant difference in surface form exists between the front and back side of the film, supporting the case that cross-linking of PEGDMA in the process of

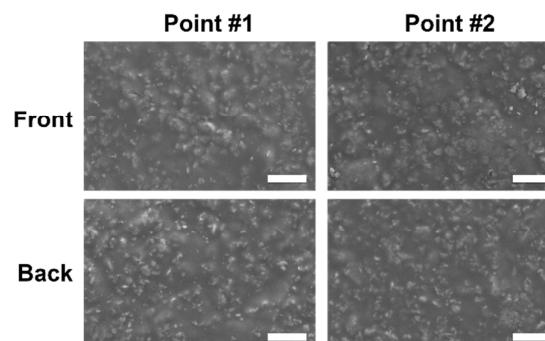


**Fig. 3.** SEM image of the front and back sides of randomly chosen two points of the vermiculite-PEG hybrid film (scale bar = 10  $\mu\text{m}$ ).

UV curing using Darocur 1173 was successfully done. SEM images of randomly chosen two points (point #1 and point #2) showed that no significant difference in surface morphology was observed. In general, the surface morphology of the film resembled the top view of the chocolate crunched balls, as some of vermiculite particles stick out of the film as some particles have a diameter between 20  $\mu\text{m}$  and 50  $\mu\text{m}$ .

To more clearly observe the morphology of the sieved vermiculite particles and their dispersion in the hybrid film, TEM images were taken, as shown in Fig. 4. Fig. 4A shows the overall morphology of sieved vermiculite particles, and Fig. 4B and Fig. 4C show their layered structure. Fig. 4D shows the dispersed sieved vermiculite particles in the vermiculite-PEG hybrid film, where the size of vermiculite particles is much smaller than that in Fig. 4A. From the TEM images, it can be concluded that sieved vermiculite particles

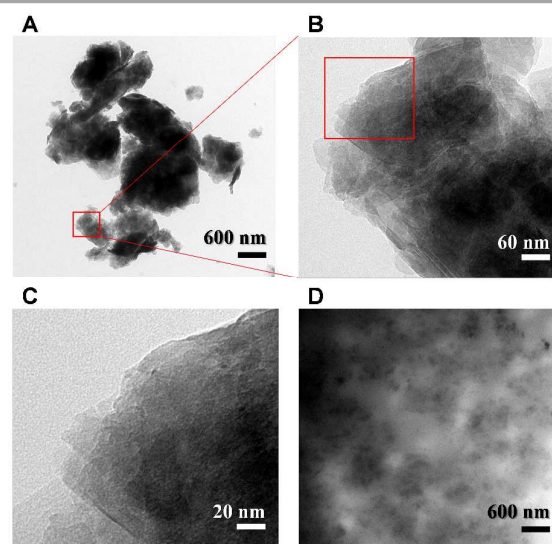


**Fig. 4.** TEM images of stacks and agglomerates of sieved vermiculite particles in relatively (A) low magnification view, (B) medium magnification view of red box in Fig. 4A, and (C) high magnification view of red box in Fig. 4B, and (D) vermiculite-PEG film (S3) with well-dispersed vermiculite particles.

*J. Name.*, 2013, **00**, 1-3 | 3

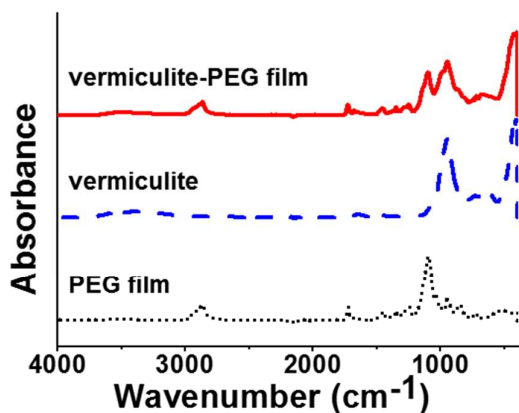


**Fig. 5.** FTIR spectrum of PEG (black, dots), vermiculite (blue, dash), and vermiculite-PEG film (S3, thickness=20  $\mu\text{m}$ , red, straight).

maintain the well-known layered structure of vermiculite and were successfully dispersed within the inorganic-polymer film.

To determine whether a new chemical bonding was formed between PEG and vermiculite within vermiculite-PEG film, FTIR analysis was conducted. The FTIR spectra of PEG film, vermiculite, and vermiculite-PEG film are presented in Fig. 5. PEG film has two prominent absorbance peaks at 1093  $\text{cm}^{-1}$  and 2866  $\text{cm}^{-1}$ ; vermiculite has two prominent absorbance peaks at 402  $\text{cm}^{-1}$  and 947  $\text{cm}^{-1}$ ; and vermiculite-PEG film has four prominent absorbance peaks at 402  $\text{cm}^{-1}$ , 946  $\text{cm}^{-1}$ , 1097  $\text{cm}^{-1}$  and 2868  $\text{cm}^{-1}$ . Such absorbance peak location suggests that no new chemical bonding was formed between vermiculite and PEG. No new absorbance peaks or significant peak shifts occurred in vermiculite-PEG film compared to the absorbance peaks of PEG film and vermiculite, indicating that no direct chemical bonding between vermiculite and PEG was formed.<sup>36,37</sup> Nevertheless, minor peak shifts of PEG and vermiculite in vermiculite-PEG hybrid film indicate that cations exposed on the surface of vermiculite could mediate reactions with PEG through metal-polymer coordination, as previous studies demonstrated that PEG has coordination reactions with different cations such as  $\text{Mg}^{2+}$ ,  $\text{Fe}^{2+}$ , and  $\text{K}^{+}$ , elements of which are present in vermiculite.<sup>38-41</sup>

The mechanical properties of vermiculite-PEG film (S2 and S3) and PEG film (control) were determined more precisely in the stress-strain curve (Fig. 6). From the stress-strain curve, the measured ultimate tensile strengths (UTS) of PEG film, S2, and S3 were 0.74 MPa, 3.64 MPa, and 4.58 MPa, respectively. Both S2 and S3 samples had higher maximum strain values before deformation, higher UTS, and longer elongation than PEG film. The vermiculite particles were well-dispersed in the cross-linked PEG network, allowing the vermiculite-PEG hybrid film also to be flexible (Fig. 7A). Slight change in color was observed among the samples of vermiculite-PEG hybrid films due to the different weight ratios of vermiculite in hybrid films (Fig. 7B). However, on a larger scheme, the SEM image of cross-section of the film shows that such stick-out is not vertically sharp. The approximate thickness of the film measured from Fig. 7C is ranged from 25  $\mu\text{m}$  to 30  $\mu\text{m}$ , which is slightly higher than the thickness measured on a Vernier caliper. Nevertheless, the thickness was measured on the Vernier caliper for its easy measurement and distinct unit difference (by 10  $\mu\text{m}$ ).

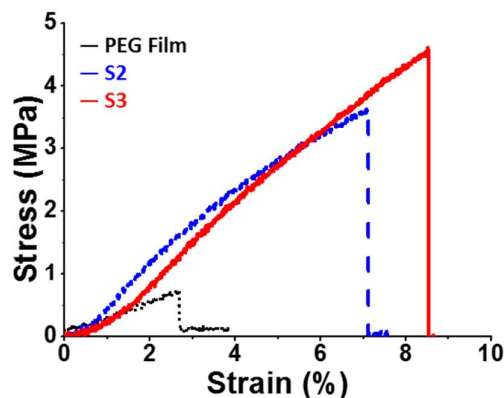


**Fig. 6.** Stress-strain curves of PEG film (black, dot), S2 (blue, dash) and S3 (red, straight) vermiculite-PEG hybrid films.

The EDX spectra of vermiculite-PEG hybrid film (S3) is presented in Fig. 8A. It was observed that earth-abundant elements such as Mg, Al, and Si were derived from the vermiculite. A small amount of C can be attributed to the presence of carbon atoms in the cross-linked PEG network. TG analysis shows that the film (S3) did not decompose wholly even at 800  $^{\circ}\text{C}$ , which is the usual temperature of the center of candle flame, and that pristine vermiculite particles undergo very small weight decomposition up to 800  $^{\circ}\text{C}$  (less than 6 wt-%) (Fig. 8B and Fig. S1). The weight loss slightly occurred from 20  $^{\circ}\text{C}$  to 200  $^{\circ}\text{C}$  (stage 1); critical weight loss then occurred from 300  $^{\circ}\text{C}$  to 450  $^{\circ}\text{C}$  (stage 2); and after that, the weight % is generally maintained until 800  $^{\circ}\text{C}$  (stage 3). These three stages can be explained in the following ways: In stage 1, slight decomposition occurred as some residues of ethanol capped inside the vermiculite-PEG film and some water contents in vermiculite

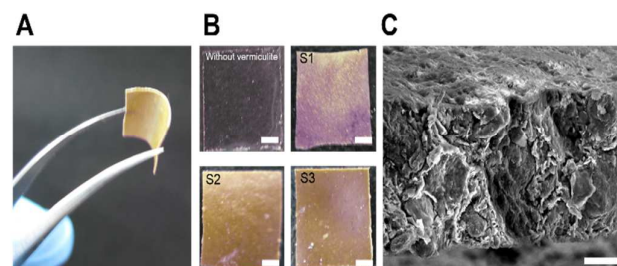


**Fig. 7.** Photographic images of (A) the fabricated vermiculite-PEG hybrid film (S3) with its flexibility and (B) different weight ratio of vermiculite hybrid films ( $1 \times 1 \text{ cm}^2$ , scale bar = 2 mm). (C) SEM image of the cross-sectional view of the vermiculite-PEG hybrid film (scale bar = 10  $\mu\text{m}$ ).

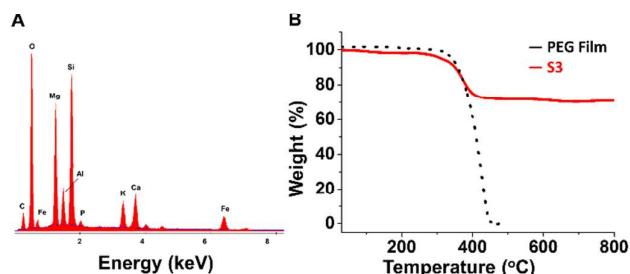


**Fig. 8.** (A) EDX spectrum and (B) TG curve of the vermiculite-PEG hybrid film (S3) and PEG film.

disappeared. Relatively sharp weight decrease of pristine vermiculite can be shown in Fig. S1 at 90 °C to 120 °C, suggesting the disappearance of minute water contents in vermiculite. For residues of ethanol, some ethanol remained as it was kept inside the gelling structure of PEG as it underwent polymerization soon before ethanol had enough time to evaporate between two glass slides. Some of ethanol was also capped inside the PEG and layered structure of vermiculite, making it difficult to be evaporated when exposed to the air condition.

In stage 2, a majority of PEG melted, as the melting point of the PEG is higher than 200 °C (Fig. 8B). The general weight loss patterns of both PEG film and S3 sample are in good agreement, suggesting that the weight loss in stage 2 is mainly attributed to the melting of PEG in a regular pattern. Such observation is also apparent in DSC curve (Fig. S2), where no melting point was observed up to 240 °C. Upon reaching 450 °C (in stage 3), almost all of PEG polymers were melted, and only the vermiculite particles remained, probably in a layered structure. Because of its complex layered structure, it remained thermally stable even at 800 °C. If one were to compare the remaining weight percentage of the film (Sample S3) at 800 °C (about 71 wt-%) and the theoretical weight of

vermiculite (74.3 wt-%), the experiments are in good agreement with the fact that most of vermiculites remained thermally stable.

The combustion behaviors of two different samples (S2 and S3), which are about 60  $\mu\text{m}$  thick, are shown in Fig. 9A. The fire flared up as the films were ignited due to the residue of ethanol inside. As expected, the S2 sample could not maintain its original structure 14 sec after ignition; on the other hands, the S3 sample endured inside of flame over 120 sec. Fig. 9B shows fire endurance data of three different samples (S1, S2, and S3). Fire endurance time was defined as the time period from the beginning of the test to the point when the weight loss of sample reached 32 wt-% (remaining weight of the sample: 68 % of the original weight of the sample before fire testing). Fire endurance time was greatly affected by the weight percentage of vermiculite added. Slight difference was observed between S1 and S2 and much larger difference in fire endurance time was observed between S2 and S3 under 60  $\mu\text{m}$  in thickness. The result clearly proves that the sample with the maximum concentration of vermiculite exhibits very favorable, thermally stable properties. On the other hand, even for the S2 sample, as the film gets thicker, fire endurance time significantly increases, especially from 80  $\mu\text{m}$  to 100  $\mu\text{m}$  and from 100  $\mu\text{m}$  to 120  $\mu\text{m}$ . The results suggest that depending on the desired thickness of the film, one does not always need to have the maximum amount of vermiculite in a solution to create a fire-retardant film.

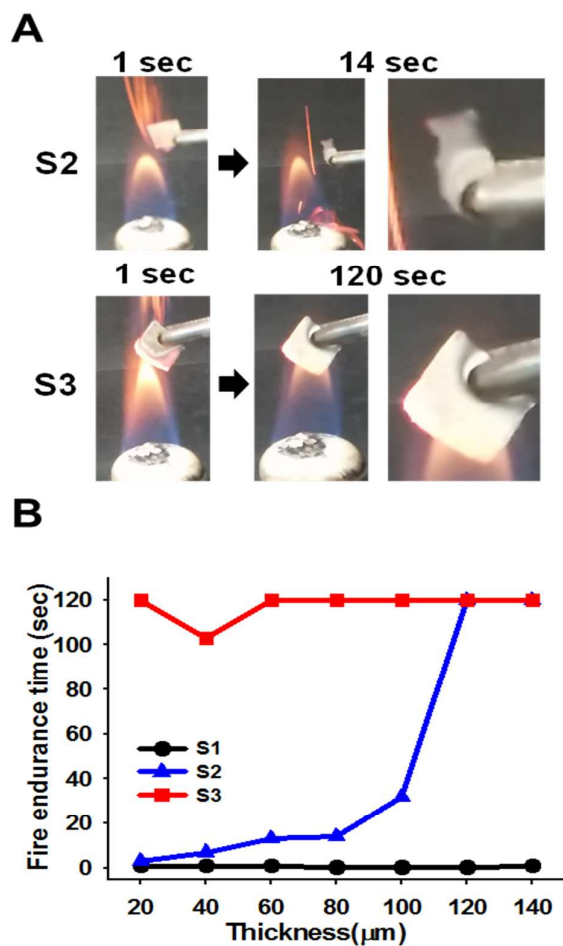


**Fig. 9.** (A) Photographic images of fire endurance tests of the vermiculite-PEG hybrid films. S2 (thickness: 60  $\mu\text{m}$ , 1 sec and 14 sec after ignition) and S3 (thickness: 60  $\mu\text{m}$ , 1 sec and 120 sec after ignition). (B) Fire endurance time of the vermiculite-PEG hybrid films, S1 (black, circle), S2 (blue, triangle), and S3 (red, rectangle).

## References

- 1 K. E.-Talway, *Journal of the Textile Institute*, 2008, **99**, 185-191.
- 2 O. Y.-Xiang, Z. Yi, H. T.-Jie, and Z. Liu, *Plastics*, 2009, **2**, 015.
- 3 T. Jana, B. C. Roy, and S. Maiti, *Polymer Degradation and Stability*, 2000, **69**, 79-82.
- 4 C. Bowen, R. Yuanlin, and K. Weimin, *Journal of Textile Research*, 2007, **28**, 19.
- 5 H. T. Deo, N. K. Patel, and B. K. Patel, *J. Eng. Fib. Fab.*, 2008, **3**, 23-38.
- 6 P. K. Sahoo and R. Samal, *Polymer Degradation and Stability*, 2007, **92**, 1700-1707.
- 7 M.-H. Ryou, Y. M. Lee, J.-K. Park, and J. W. Choi, *Advanced Materials*, 2011, **23**, 3066-3070.
- 8 J. A. Scheffer, *Industrial & Engineering Chemistry*, 1935, **27**, 1298-1303.
- 9 S. A. Suvorov and V. V. Skurikhin, *Refractories and Industrial Ceramics*, 2003, **44**, 186-193.
- 10 J. Addison, *Regulatory Toxicology and Pharmacology*, 1995, **21**, 397-405.
- 11 S. Takahashi, H. A. Goldberg, C. A. Feeney, D. P. Karim, M. Farrell, K. O'Leary, and D. R. Paul, *Polymer*, 2006, **47**, 3083-3093.
- 12 A. A. Cain, M. G. Plummer, S. E. Murray, L. Bolling, O. Regev, and J. C. Grunlan, *Journal of Materials Chemistry A*, 2014, **2**, 17609.
- 13 O. Abollino, A. Giacomino, M. Malandrino, and E. Mentasti, *Water Air Soil Pollut*, 2007, **181**, 149-160.
- 14 A. Karaipekli and A. Sari, *Solar Energy*, 2009, **83**, 323-332.
- 15 N. Khandaker and P. Seto, *International Journal of Green Energy*, 2010, **7**, 38-42.
- 16 M. Malandrino, O. Abollino, S. Buoso, A. Giacomino, C. L. Gioia, and E. Mentasti, *Chemosphere*, 2011, **82**, 169-178.
- 17 J. Yu, J. He, and C. Ya, *Journal of Applied Polymer Science*, 2011, **119**, 275-281.
- 18 J. Drelich, B. Li, P. Bowen, J.-Y. Hwang, O. Mills, and D. Hoffman, *Applied Surface Science*, 2011, **257**, 9435-9443.
- 19 F. Koksall, O. Gencel, W. Brostow, H. E. H. Lobland, *Materials Research Innovations*, 2012, **16**, 7-13.
- 20 P. Wu, C. Liu, Z. Huang, W. Wang, *RSC Advances*, 2014, **4**, 25580.
- 21 C. A. Alexiades and M. L. Jackson, *Soil Science Society of America Journal*, 1965, **29**, 522-527.
- 22 W. A. Adams and J. K. Kassim, *Soil Science Society of America Journal*, 1983, **47**, 316-320.
- 23 R. H. April, M. M. Hluchy, and R. M. Newton, *Clays and Clay Minerals*, 1986, **34**, 549-556.
- 24 R. Kozlowski, B. Mieleniak, and M. Helwig, *Polymer Degradation and Stability*, 1999, **64**, 523-528.
- 25 J. E. Connell, E. Metcalfe, and M. J. Thomas, *Polym. Int.*, 2000, **49**, 1092-1094.
- 26 M. Zanetti, G. Camino, D. Canavese, A. B. Morgan, F. J. Lamelas, and C. A. Wilkie, *Chem. Mater.*, 2002, **14**, 189-193.
- 27 S. C. Tjong, Y. Z. Meng, and A. S. Hay, *Chem. Mater.*, 2002, **14**, 44-51.
- 28 S. Chen, B. Wang, J. Kang, J. Chen, J. Gai, L. Yang, Y. Cao, *Journal of Macromolecular Science B*, 2014, **52**, 1212-1225.
- 29 W. A. W. Zaharuddin, B. Ariwahjoedi, and P. Hussain, *Journal of Applied Sciences*, 2011, **11**, 1763-1769.
- 30 L. A. Peipins, M. Lewin, S. Campolucci, J. A. Lybarger, A. Miller, D. Middleton, C. Weis, M. Spence, B. Black, and V. Kapil, *Environmental Health Perspectives*, 2003, **111**, 1753.
- 31 P. A. Sullivan, *Environmental Health Perspectives*, 2007, **115**, 579.
- 32 J. C. McDonald, A. D. McDonald, B. Armstrong, and P. Sebastien, *British Journal of Industrial Medicine*, 1986, **43**, 436-444.
- 33 J. C. McDonald, J. Harris, and B. Armstrong. *Occup Environ Med*, 2004, **61**, 363-366.
- 34 S. Backstrom, J. Benavente, R. W. Berg, K. Stibius, M. S. Larsen, H. Bohr, and C. H. Nielson, *Materials Sciences and Applications*, 2012, **3**, 425-431.
- 35 C. N. Bowman, A. L. Carver, S. L. Kennett, M. M. Williams, and N. A. Peppas, *Polymer Bulletin*, 1988, **20**, 329-333.
- 36 S.-D. Jiang, G. Tang, Z.-M. Bai, Y.Y. Wang, and L. Song, *RSC Advances*, 2014, **4**, 3253.
- 37 S. Karaman, A. Karaipekli, A. Sari, and A. Bicer, *Solar Energy Materials & Solar Cells*, 2011, **95**, 1647-1653.
- 38 V. D. Noto, *J. Phys. Chem. B*, 2002, **106**, 11139-11154.
- 39 M. Piccolo, G. A. Giffin, K. Vezzu, F. Bertasi, P. Alotto, M. Guarnieri, and V. D. Noto, *ChemSusChem*, 2013, **6**, 2157-2160.
- 40 G. L. Fiore, J. L. Klinkenberg, A. Pfister, and C. L. Fraser, *Biomacromolecules*, 2009, **10**, 128-133.
- 41 A. Zalewska, J. Stygar, E. Ciszewska, M. Wiktorko, and W. Wieczorek, *J. Phys. Chem. B*, 2001, **105**, 5847-5851.